NLO QCD effective field theory analysis of W^{+}W^{-} production at the LHC including fermionic operators

Julien Baglio, Sally Dawson, and Ian M. Lewis

Phys. Rev. D **96**, 073003 — Published 3 October 2017

DOI: 10.1103/PhysRevD.96.073003

An NLO QCD effective field theory analysis of W^+W^- production at the LHC including fermionic operators

Julien Baglio,[1,*] Sally Dawson,[2,†] and Ian M. Lewis[3,‡]

[1] *Institute for Theoretical Physics, University of Tübingen, Auf der Morgenstelle 14, 72076 Tübingen, Germany*

[2] *Department of Physics, Brookhaven National Laboratory, Upton, N.Y., 11973 U.S.A.*

[3] *Department of Physics and Astronomy, University of Kansas, Lawrence, Kansas, 66045 U.S.A.*

Abstract

We study the impact of anomalous gauge boson and fermion couplings on the production of W^+W^- pairs at the LHC. Helicity amplitudes are presented separately to demonstrate the sources of new physics contributions and the impact of QCD and electroweak corrections. The QCD corrections have important effects on the fits to anomalous couplings, in particular when one W boson is longitudinally polarized and the other is transversely polarized. In effective field theory language, we demonstrate that the dimension-6 approximation to constraining new physics effects in W^+W^- pair production fails at $p_T \sim 500 - 1000$ GeV.

*Electronic address: julien.baglio@uni-tuebingen.de

†Electronic address: dawson@bnl.gov

‡Electronic address: ian.lewis@ku.edu

I. INTRODUCTION

The $SU(2)\times U(1)$ structure of the electroweak sector of the Standard Model completely determines the W^+W^-V interactions ($V=\gamma, Z$). The amplitudes for the production of W^+W^- pairs involve subtle cancellations between contributions that grow with energy, and individual Feynman diagrams violate perturbative unitarity [1–3]. In models with new high scale physics, the form of these interactions can be changed, potentially spoiling the cancellations that impose unitarity conservation, and so the pair production of gauge bosons can be extremely sensitive to new physics interactions, providing a stringent test of the Standard Model (SM). Precision constraints on anomalous 3−gauge boson couplings have been found from $e^+e^- \to W^+W^-$ measurements at LEP-II [4], and even stronger constraints have been derived at the LHC from W^+W^- production [5–9]. The experimental analyses [10, 11], however, assume that all the new physics is in the 3−gauge boson couplings. In principle, both the fermion couplings to Z bosons and W bosons could be altered, changing the results of the fits to new physics contributions [5, 7, 9]. Although the Z−fermion couplings are highly constrained by LEP data, they can still have numerically significant effects on the fit to W^+W^- pair production.

A consistent theoretical analysis requires the use of effective Lagrangian techniques. The new physics is parameterized as an operator expansion in inverse powers of the high scale, Λ, where the new physics is assumed to occur,

$$\mathcal{L}_{\rm SMEFT} = \mathcal{L} \sim \mathcal{L}_{\rm SM} + \sum_{i,n} \frac{C_i^{(n)}}{\Lambda^{n-4}} O_i^{(n)} + \dots \tag{1}$$

where $O_i^{(n)}$ has mass dimension-n and $\mathcal{L}_{\rm SM}$ contains the complete SM Lagrangian. Neglecting flavor, there are 59 possible operators at dimension-6 [12, 13], but only a small subset contribute to W^+W^- production. The goal of this work is to consistently extract limits on potential new physics effects in pair production of W^+W^- at the LHC, including modifications to both three-gauge-boson vertices and fermion−gauge-boson vertices. We first review the effects of non-SM interactions in the various helicity channels, since the W^+W^- helicity amplitudes have differing behaviors at high energy, which may facilitate the extraction of anomalous couplings [1–3, 14, 15].

The effects of new physics contributions to gauge boson pair production can be expected to be of the same order of magnitude as QCD and electroweak (EW) corrections,

and so these contributions must be included when extracting limits on new physics. The SM QCD corrections to W^+W^- pair production are known to NNLO [16, 17], including the effects of a jet veto [18, 19]. The EW corrections are typically small [20–22], and the combined QCD/EW corrections including leptonic W decays have been implemented [23–25]. We perform an analysis including QCD [26] and EW corrections [21], along with modifications of both the three-gauge-boson and fermion couplings. Section II reviews the formalism of anomalous couplings in W^+W^- pair production and lowest order (LO) and next-to-leading order (NLO) results are presented in Sections III A and III B. Section IV contains some conclusions about the impact of our work on fits to anomalous couplings.

II. BASICS

Assuming CP conservation, the most general Lorentz invariant 3−gauge boson couplings can be written as [1, 3]

$$\mathcal{L}_V = -ig_{WWV}\left(g_1^V\left(W^+_{\mu\nu}W^{-\mu}V^\nu - W^-_{\mu\nu}W^{+\mu}V^\nu\right) + \kappa^V W^+_\mu W^-_\nu V^{\mu\nu} + \frac{\lambda^V}{M_W^2}W^+_{\rho\mu}W^{-\mu}{}_\nu V^{\nu\rho}\right) \quad (2)$$

where $V = \gamma, Z$ and $g_{WW\gamma} = e$ and $g_{WWZ} = g\cos\theta_W$, θ_W being the weak mixing angle. We use the abbreviations $s_W \equiv \sin\theta_W$ and $c_W \equiv \cos\theta_W$. The fields in Eq.(2) are the canonically normalized mass eigenstate fields. In a similar fashion, we define the effective couplings of fermions to gauge fields and assume that the structure of the charged and neutral currents is that of the SM[1],

$$\begin{aligned}\mathcal{L} \;=\; & g_Z Z_\mu\left[g_L^{Zq} + \delta g_L^{Zq}\right]\overline{q}_L\gamma_\mu q_L \;+ g_Z Z_\mu\left[g_R^{Zq} + \delta g_R^{Zq}\right]\overline{q}_R\gamma_\mu q_R \\ & + \frac{g}{\sqrt{2}}\left\{W_\mu\left[(1+\delta g_L^W)\overline{q}_L\gamma_\mu q'_L + \delta g_R^W\overline{q}_R\gamma_\mu q'_R\right] + h.c.\right\}, \end{aligned} \quad (3)$$

where $g_Z = e/(c_W s_W) \equiv g/c_W$, Q_q is the electric charge of the quarks, and q denotes up-type or down-type quarks. The SM quark couplings are:

$$g_R^{Zq} \;=\; -s_W^2 Q_q \quad \text{and} \quad g_L^{Zq} = T_3^q - s_W^2 Q_q, \quad (4)$$

[1] Dipole operators change the structure of the charged and neutral currents. However, the dipole contributions appear at dimension-8 in the amplitude squared since they do not interfere with the SM. Hence, we neglect them.

where $T_3^q = \pm\frac{1}{2}$. For the 3−gauge boson couplings we define $g_1^V = 1+\delta g_1^V$, $\kappa^V = 1+\delta\kappa^V$, and in the SM $\delta g_1^V = \delta\kappa^V = \lambda^V = 0$. Because of gauge invariance we always have $\delta g_1^\gamma = 0$. We assume $SU(2)$ invariance, which relates the coefficients,

$$\begin{aligned} \delta g_L^W &= \delta g_L^{Zf} - \delta g_L^{Zf'}, \\ \delta g_1^Z &= \delta\kappa^Z + \frac{s_W^2}{c_W^2}\delta\kappa^\gamma, \\ \lambda^\gamma &= \lambda^Z, \end{aligned} \tag{5}$$

where f denotes up-type quarks and f' down-type quarks.

The helicity amplitudes for $q\overline{q} \to W^+W^-$ have been derived in many places [1, 3, 14, 15], and we summarize the results in Appendix A. In the high energy limit, $s \gg M_Z^2$, the SM amplitude has the behavior $\mathcal{A}(q\overline{q} \to W^+W^-) \sim \mathcal{O}(1)$. In the presence of anomalous couplings, the leading contribution in the high energy limit comes from the longitudinal gauge boson amplitudes, resulting from the interference of the SM amplitudes with the non-SM contribution. The amplitude $\mathcal{A}_{ss'\lambda\lambda'}$ for $\overline{q}_s q_{s'} \to W_\lambda^+ W_{\lambda'}^-$, where s, s', λ, λ' label the respective particle helicities, has the high energy limit,

$$\begin{aligned} \mathcal{A}_{+-00} &\to \frac{g^2 s}{2M_W^2}\sin\theta\left\{\delta\kappa^Z\left(s_W^2 Q_q - T_3^q\right) - s_W^2 Q_q\delta\kappa^\gamma - \delta g_L^{Zq} + 2T_3^q\delta g_L^W\right\}, \\ \mathcal{A}_{-+00} &\to \frac{g^2 s}{2M_W^2}\sin\theta\left\{s_W^2 Q_q\left(\delta\kappa^\gamma - \delta\kappa^Z\right) + \delta g_R^{Zq}\right\}. \end{aligned} \tag{6}$$

We have retained only the linear contribution from the anomalous couplings here and θ is the angle between the beam axis and the gauge boson direction in the center-of-mass system. At high energies the longitudinal amplitude coming from the non-SM couplings is enhanced and is $\mathcal{O}(s/M_W^2)$, while the SM amplitude for longitudinal W^+W^- production is $\mathcal{O}(1)$. Hence, the interference between SM and anomalous couplings is $\mathcal{O}(s/M_W^2)$ and grows with energy.

The SM and anomalous amplitudes for producing 2− transverse W bosons with opposite helicities in the $\overline{q}_+ q_- \to W_\pm^+ W_\mp^-$ configurations are $\mathcal{O}(1)$, while the SM amplitudes with same helicity W bosons in the $\overline{q}_+ q_- \to W_\pm^+ W_\pm^-$ configurations are $\mathcal{O}(M_W^2/s)$ and the leading term from the anomalous couplings is,

$$\mathcal{A}_{+-\pm\pm} \to -g^2\lambda^Z T_3^q \frac{s}{2M_W^2}\sin\theta, \tag{7}$$

leading to a growth at high energies in the transverse amplitude in the presence of non-zero λ^Z. The configurations with right-handed quarks with same helicity W bosons, $\overline{q}_- q_+ \to W^+_\pm W^-_\pm$, are $\mathcal{O}(1)$ and opposite helicity Ws, $\overline{q}_- q_+ \to W^+_\pm W^-_\mp$, are zero. Following this discussion, even though the anomalous coupling amplitude grows with energy, it is clear that the interference between SM and anomalous couplings is at most $\mathcal{O}(1)$.

Finally, the SM amplitude for producing one longitudinal and one transverse gauge boson is suppressed by $M_W/\sqrt{s}$, while the contribution from anomalous couplings is $\mathcal{O}(\sqrt{s}/M_W)$, making this channel also quite sensitive to anomalous couplings,

$$\begin{aligned}
\mathcal{A}_{+-0\mp} = \mathcal{A}_{+-\pm 0} \;\to\; & \frac{g^2\sqrt{s}}{\sqrt{2}M_W}(1 \pm \cos\theta)\Bigg\{\delta g_L^{Zq} - 2T_3^q \delta g_L^W + \frac{T_3^q}{2}\left(2\delta g_1^Z + \lambda^Z - \frac{s_W^2}{c_W^2}\delta\kappa^\gamma\right) + \\
& \frac{s_W^2 Q_q}{2}\left(\frac{\delta\kappa^\gamma}{c_W^2} - 2\delta g_1^Z\right)\Bigg\}, \\
\mathcal{A}_{-+0\mp} = \mathcal{A}_{-+\pm 0} \;\to\; & \frac{g^2\sqrt{s}}{\sqrt{2}M_W}(1 \mp \cos\theta)\left\{\delta g_R^{Zq} + \frac{s_W^2 Q_q}{2}\left(\frac{\delta\kappa^\gamma}{c_W^2} - 2\delta g_1^Z\right)\right\}. \qquad (8)
\end{aligned}$$

As with the the two transverse W case, when one W is transverse and the other longitudinal the interference between SM and anomalous couplings is $\mathcal{O}(1)$.

The Lagrangians of Eqs.(2) and (3) can be mapped onto the effective Lagrangian (EFT) of Eq.(1), where we work to dimension-6, assuming that the scale Λ is much larger than the weak scale, and that the couplings C_i are perturbative. For simplicity, we work in the Warsaw basis [13] and the dimension-6 operators relevant for our analysis are,

$$\begin{aligned}
\mathcal{O}_{3W} &= \epsilon^{abc} W_\mu^{a\nu} W_\nu^{b\rho} W_\rho^{c\mu}, \\
\mathcal{O}_{HD} &= |\, \Phi^\dagger (D_\mu \Phi)\, |^2, \\
\mathcal{O}_{HWB} &= \Phi^\dagger \sigma^a \Phi W^a_{\mu\nu} B^{\mu\nu} \\
\mathcal{O}^{(3)}_{HF} &= i\left(\Phi^\dagger \overleftrightarrow{D}^a_\mu \Phi\right)\overline{f}_L \gamma^\mu \sigma^a f_L, \\
\mathcal{O}^{(1)}_{HF} &= i\left(\Phi^\dagger \overleftrightarrow{D}_\mu \Phi\right)\overline{f}_L \gamma^\mu f_L, \\
\mathcal{O}_{Hf} &= i\left(\Phi^\dagger \overleftrightarrow{D}_\mu \Phi\right)\overline{q}_R \gamma^\mu q_R, \\
\mathcal{O}_{Hud} &= i\left(\widetilde{\Phi}^\dagger D_\mu \Phi\right)\overline{u}_R \gamma^\mu d_R, \\
\mathcal{O}_{ll} &= (\bar{l}_L \gamma^\mu l_L)(\bar{l}_L \gamma_\mu l_L), \qquad (9)
\end{aligned}$$

where $D_\mu \Phi = (\partial_\mu - i\,\frac{g}{2}\sigma^a W^a_\mu - i\frac{g'}{2}B_\mu)\Phi$, $W^a_{\mu\nu} = \partial_\mu W^a_\nu - \partial_\nu W^a_\mu + g\varepsilon^{abc} W^b_\mu W^c_\nu$, $\Phi^\dagger \overleftrightarrow{D}_\mu \Phi = \Phi^\dagger D_\mu \Phi - (D_\mu \Phi^\dagger)\Phi$, and $\Phi^\dagger \overleftrightarrow{D}^a_\mu \Phi = \Phi^\dagger D_\mu \sigma^a \Phi - (D_\mu \Phi^\dagger)\sigma^a \Phi$. Φ stands for the Higgs doublet

field with a vacuum expectation value $\langle\Phi\rangle = (0, v/\sqrt{2})^{\rm T}$. The Lagrangian of Eq.(1) introduces non-canonically normalized gauge fields. The input parameters we choose for our analysis are $G_F = 1.16637\times10^{-5}$ GeV^{-2}, $M_Z = 91.1876$ GeV and $M_W = 80.385$ GeV, taken from their experimental values. In the mapping from EFT operators to anomalous couplings we have to take into account the EFT shifts $g_Z \to g_Z + \delta g_Z$, $v \to v(1+\delta v)$, $s_W^2 \to s_W^2 + \delta s_W^2$ in the definition of the model input parameters for the gauge couplings, as well as for s_W, so that we get back to canonically normalized gauge fields. This gives [27, 28]

$$\begin{aligned}
\delta v &= C_{Hl}^{(3)} - \frac{1}{2}C_{ll},\\
\delta g_Z &= -\frac{v^2}{\Lambda^2}\left(\delta v + \frac{1}{4}C_{HD}\right),\\
\delta s_W^2 &= -\frac{v^2}{\Lambda^2}\frac{s_W c_W}{c_W^2 - s_W^2}\left[2 s_W c_W\left(\delta v + \frac{1}{4}C_{HD}\right) + C_{HWB}\right],
\end{aligned} \tag{10}$$

where the tree-level relations are still valid:

$$v^2 = \frac{1}{\sqrt{2}G_F}, \quad s_W^2 = 1 - \frac{M_W^2}{M_Z^2}, \quad g_Z = \frac{2M_Z}{v} = \frac{g}{c_W} = \frac{e}{c_W s_W}. \tag{11}$$

Using these shifts and the operators defined in Eq.(9) we find the following mapping,

$$\begin{aligned}
\delta g_1^Z &= \frac{v^2}{\Lambda^2}\frac{1}{c_W^2 - s_W^2}\left(\frac{s_W}{c_W}C_{HWB} + \frac{1}{4}C_{HD} + \delta v\right),\\
\delta\kappa^Z &= \frac{v^2}{\Lambda^2}\frac{1}{c_W^2 - s_W^2}\left(2 s_W c_W C_{HWB} + \frac{1}{4}C_{HD} + \delta v\right),\\
\delta\kappa^\gamma &= -\frac{v^2}{\Lambda^2}\frac{c_W}{s_W}C_{HWB},\\
\lambda^\gamma &= \frac{v}{\Lambda^2}3M_W C_{3W},\\
\lambda^Z &= \frac{v}{\Lambda^2}3M_W C_{3W},\\
\delta g_L^W &= \frac{v^2}{\Lambda^2}C_{Hq}^{(3)} + c_W^2\delta g_Z + \delta s_W^2,\\
\delta g_R^W &= \frac{v^2}{2\Lambda^2}C_{Hud}\\
\delta g_L^{Zu} &= -\frac{v^2}{2\Lambda^2}\left(C_{Hq}^{(1)} - C_{Hq}^{(3)}\right) + \frac{1}{2}\delta g_Z + \frac{2}{3}\left(\delta s_W^2 - s_W^2\delta g_Z\right),\\
\delta g_L^{Zd} &= -\frac{v^2}{2\Lambda^2}\left(C_{Hq}^{(1)} + C_{Hq}^{(3)}\right) - \frac{1}{2}\delta g_Z - \frac{1}{3}\left(\delta s_W^2 - s_W^2\delta g_Z\right),\\
\delta g_R^{Zu} &= -\frac{v^2}{2\Lambda^2}C_{Hu} + \frac{2}{3}\left(\delta s_W^2 - s_W^2\delta g_Z\right),\\
\delta g_R^{Zd} &= -\frac{v^2}{2\Lambda^2}C_{Hd} - \frac{1}{3}\left(\delta s_W^2 - s_W^2\delta g_Z\right),
\end{aligned} \tag{12}$$

in agreement with Refs. [9, 29]

The operator $\mathcal{O}_{Hud}$ can mediate sources of flavor violation in addition to the SM. To suppress this new source, we work under the assumption of minimal flavor violation (MFV) [30, 31]: all flavor violation is generated via the Yukawa matrices. Under this assumption $C_{Hud} \sim Y_u Y_d$, where Y_u and Y_d are up- and down-quark Yukawa matrices, respectively [32]. Hence, for light initial state quarks we can safely assume $\delta g_R^W = 0$. Additionally, $C_{Hq}^{(3)}$, $C_{Hq}^{(1)}$, and C_{Hf} are assumed to be flavor diagonal and universal.

The amplitude for W^+W^- production is generically written as,

$$\mathcal{A} \sim \mathcal{A}_{\rm SM} + \frac{1}{\Lambda^2}\mathcal{A}_{\rm EFT} + \dots \tag{13}$$

In a consistent EFT approach, one should keep only the contributions to the cross section proportional to $1/\Lambda^2$, and so the amplitude-squared is,

$$\sigma \sim \frac{1}{s}\left(\mid \mathcal{A}_{\rm SM} \mid^2 + \mathcal{A}_{\rm SM}^* \frac{\mathcal{A}_{\rm EFT}}{\Lambda^2} + \dots \right) \tag{14}$$

Dropping the $1/\Lambda^4$ terms (and beyond) means that the cross section is not guaranteed to be positive and the region of validity of the EFT is hence restricted [33]. We will discuss this in detail in the next section.

III. NUMERICAL RESULTS

A. Lowest order and NLO electroweak effects

It is well known that both anomalous fermion couplings and non-SM three gauge boson couplings lead to cross sections which grow at high energy, Eq.(6). By fitting to the deviation of the high p_T spectrum from the SM prediction, limits are obtained on the size of the anomalous couplings. Both ATLAS and CMS [34] have searched for anomalous triple gauge boson couplings at the 8 TeV LHC. Using the ATLAS bounds on the anomalous triple gauge boson couplings, at leading order we determine a range of the cross section

$$\sigma_{\rm min}^{\rm cut} < \sigma^{\rm cut} \equiv \sigma(p_T^{W^+} > 500 \text{ GeV}) = \int_{500 \text{ GeV}}^{\infty} dp_T^{W^+} \frac{d\sigma}{dp_T^{W^+}} < \sigma_{\rm max}^{\rm cut} \ , \tag{15}$$

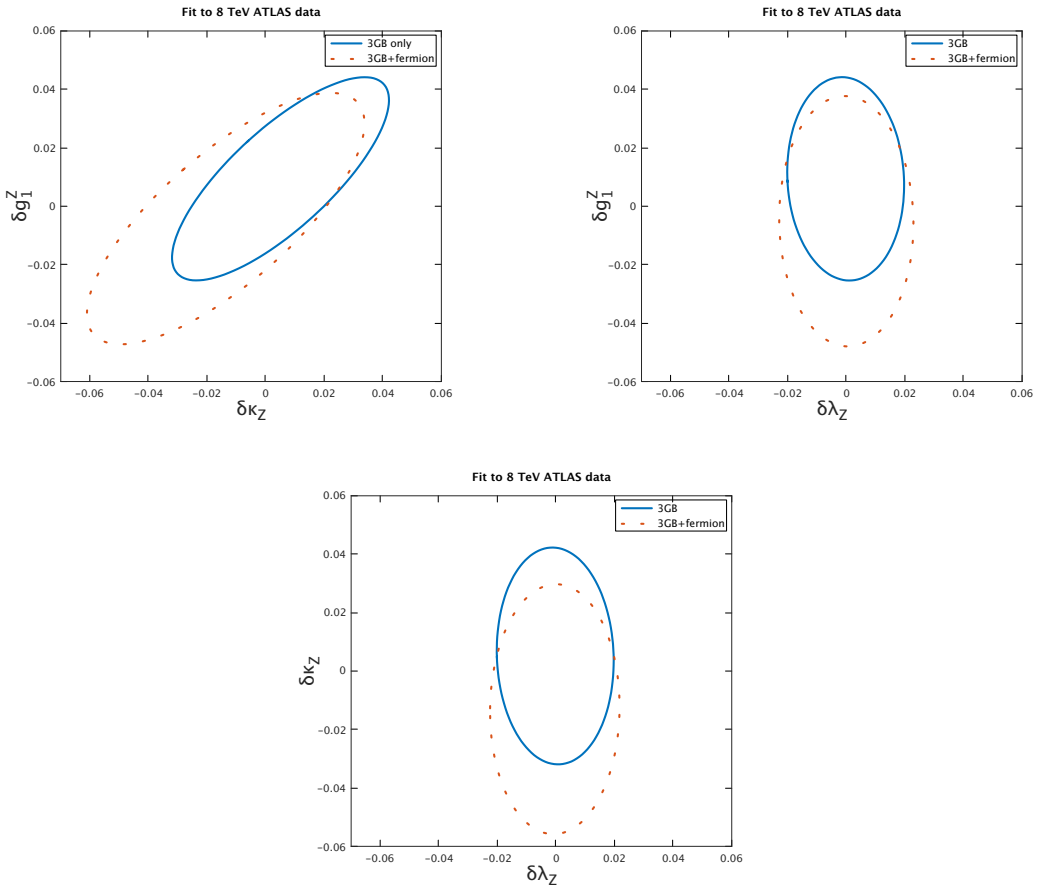

FIG. 1: Results of a parameter scan over (red dashed lines) anomalous triple gauge boson and fermion couplings and (solid blue lines) anomalous triple gauge boson couplings with fermion couplings set to their SM values. The allowed regions are inside the ellipses.

where $\sigma = \sigma(pp \to W^+W^-)$ is the W^+W^- hadronic production cross section and $p_T^{W^+}$ is the W^+ transverse momentum[2]. It is assumed that any $\sigma^{\rm cut}$ above $\sigma^{\rm cut}_{\rm max}$ or below $\sigma^{\rm cut}_{\rm min}$ would have been observable and any point violating these bounds is rejected. Using this technique, we reproduce both the ATLAS and CMS bounds on anomalous 3−gauge boson couplings. Next, we perform a scan over all anomalous triple gauge boson couplings and fermion couplings. The anomalous fermion couplings in our scan are constrained by LEP

[2] We use the complete $\mid A \mid^2$ for the scans.

limits [5]:

$$\begin{aligned}
\delta g_L^{Zu} &= (-2.6 \pm 1.6) \times 10^{-3}, \\
\delta g_L^{Zd} &= (2.3 \pm 1) \times 10^{-3}, \\
\delta g_R^{Zu} &= (-3.6 \pm 3.5) \times 10^{-3}, \\
\delta g_R^{Zd} &= (16.0 \pm 5.2) \times 10^{-3}.
\end{aligned} \tag{16}$$

The results of these scans are shown in Fig. 1; the allowed regions are within the ellipses[3]. The blue lines consider only anomalous triple gauge boson couplings with fermion couplings set to the SM values. These results are consistent with the ATLAS results. The red lines consider both non-zero anomalous triple gauge boson and anomalous fermion couplings. As can be seen, by including the anomalous fermion couplings the central values of the allowed parameters change and the areas of the allowed regions increase[4]. Although LEP constrains them to be very small, the importance of the anomalous fermion couplings is already apparent. We have checked that these results are stable against changes in the $p_T^{W^+}$ lower bound in Eq.(15).

We consider two representative scenarios, allowed by global fits to anomalous fermion couplings and anomalous 3-gauge-boson couplings [5, 7, 36] both at the same time. The scenarios we consider are:

$$\begin{aligned}
\text{3GB}: \quad & \delta g_1^Z = 0.0163,\ \delta\kappa^Z = 0.0239,\ \lambda^Z = 0.00452, \\
\text{Ferm}: \quad & \delta g_L^{Zu} = -0.00239,\ \delta g_R^{Zu} = -0.0069, \\
& \delta g_L^{Zd} = 0.00271,\ \delta g_R^{Zd} = 0.0212.
\end{aligned} \tag{17}$$

In addition, δg_L^W, λ^γ, and $\delta\kappa^\gamma$ are determined by the relations from Eq.(5), and δg_R^W is set to zero according to our MFV assumption. In the "3GB" scenario we set the fermionic anomalous couplings to zero (only the three-gauge-boson anomalous couplings are considered), while in the "Ferm" scenario we set the three-gauge-boson anomalous couplings to zero (only the fermionic anomalous couplings are considered). The anomalous couplings of Eq.(17) can be translated to the EFT Wilson coefficients using Eq.(12) for the two scenarios considered. In the "Ferm" scenario we have in general $C_{HWB} = C_{3W} = 0$ as

[3] The ellipses were determined using the Khachiyan Algorithm as implemented in Ref. [35].
[4] Fits to CMS W^+W^- data lead to similar conclusions.

well as $C_{HD} = 2C_{ll} - 4C_{Hl}^{(3)}$, while for the "3GB" scenario all coefficients are in principle non-zero in our operator basis and have the following relations,

$$\begin{aligned} C_{Hu} &= 4C_{Hq}^{(1)},\ C_{Hd} = -2C_{Hq}^{(1)}, \\ C_{Hq}^{(3)} &= \frac{c_W s_W}{c_W^2 - s_W^2}\left\{C_{HWB} + \frac{c_W}{s_W}\left(\frac{1}{4}C_{HD} + C_{Hl}^{(3)} - \frac{1}{2}C_{ll}\right)\right\}. \end{aligned} \tag{18}$$

We obtain the following Wilson coefficients in the "3GB" scenario,

$$\begin{aligned} \frac{1}{\Lambda^2}\left(C_{Hl}^{(3)} - \frac{1}{2}C_{ll} + \frac{1}{4}C_{HD}\right) &= 2.36 \times 10^{-8}\ \text{GeV}^{-2}, \\ \frac{C_{3W}}{\Lambda^2} = 7.61 \times 10^{-8}\ \text{GeV}^{-2},\ \frac{C_{HWB}}{\Lambda^2} &= 2.34 \times 10^{-7}\ \text{GeV}^{-2}, \\ \frac{C_{Hq}^{(1)}}{\Lambda^2} = -6.18 \times 10^{-8}\ \text{GeV}^{-2},\ \frac{C_{Hq}^{(3)}}{\Lambda^2} &= 2.09 \times 10^{-7}\ \text{GeV}^{-2}, \\ \frac{C_{Hu}}{\Lambda^2} = -2.47 \times 10^{-7}\ \text{GeV}^{-2},\ \frac{C_{Hd}}{\Lambda^2} &= 1.24 \times 10^{-7}\ \text{GeV}^{-2}, \end{aligned} \tag{19}$$

and we obtain the following Wilson coefficients in the "Ferm" scenario,

$$\begin{aligned} \frac{1}{\Lambda^2}\left(C_{Hl}^{(3)} - \frac{1}{2}C_{ll} + \frac{1}{4}C_{HD}\right) &= 0, \\ \frac{C_{3W}}{\Lambda^2} = \frac{C_{HWB}}{\Lambda^2} &= 0, \\ \frac{C_{Hq}^{(1)}}{\Lambda^2} = -5.28 \times 10^{-9}\ \text{GeV}^{-2}\ ,\ \frac{C_{Hq}^{(3)}}{\Lambda^2} &= -8.41 \times 10^{-8}\ \text{GeV}^{-2}, \\ \frac{C_{Hu}}{\Lambda^2} = 2.28 \times 10^{-7}\ \text{GeV}^{-2}\ ,\ \frac{C_{Hd}}{\Lambda^2} &= -6.99 \times 10^{-7}\ \text{GeV}^{-2}. \end{aligned} \tag{20}$$

Assuming that all C_i are perturbative ($C_i \lesssim 1$), the lower bound on the EFT scale is $\Lambda \gtrsim 2.8$ TeV.

In Figs. 2 and 3, we show the tree-level cross sections for transverse-transverse (TT), transverse-longitudinal (TL+LT or simply LT), and longitudinal-longitudinal (LL) W^+W^- polarizations, along with the sum over polarizations. We use CT14QED_inc PDFs [37] implemented via LHAPDF [38], and set the renormalization and factorization scales to be M_W. For the anomalous coupling scenarios, we present both the amplitude-squared using the amplitudes given in Appendix A, and the EFT result consistently truncated at $\mathcal{O}(1/\Lambda^2)$. The TT amplitude is by far the largest contribution to the SM rate. As shown in the left-hand side (LHS) of Fig. 2, the $W_T^+W_T^-$ rates in our anomalous coupling scenarios are indistinguishable from the SM when truncating at $\mathcal{O}(1/\Lambda^2)$; the

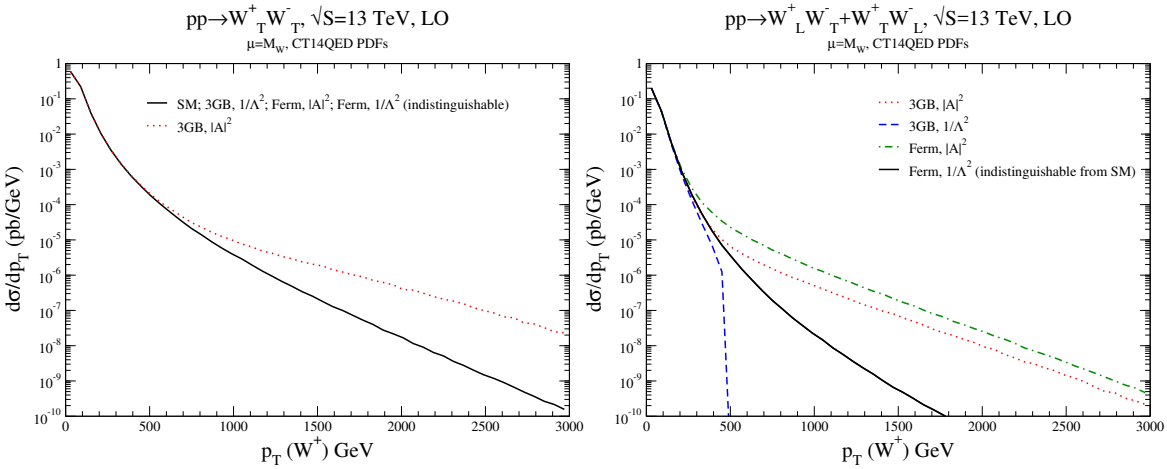

FIG. 2: Tree-level cross sections for $W_T^+W_T^-$ (LHS) and $W_T^+W_L^- + W_L^+W_T^-$ (RHS) production at the 13 TeV LHC in the SM and in the scenarios of Eq.(17). The curves labelled $|A|^2$ include the square of the dimension-6 amplitudes, while the curves labelled $1/\Lambda^2$ have the EFT result consistently truncated at $1/\Lambda^2$. The LT curve (RHS) for the 3GB amplitude in the EFT should be truncated at $p_T \sim 500$ GeV, where the LT rate becomes negative and the EFT expansion fails.

complete effect of the 3GB anomalous couplings (red line on the LHS of Fig. 2) comes from the square of the anomalous coupling contribution. The growth of the TT amplitude with energy is due to the non-zero $\lambda^\gamma = \lambda^Z$ (C_{3W}). The right-hand side (RHS) of Fig. 2 has the contribution from $W_L^\pm W_T^\mp$ production. The "3GB" scenario shows the EFT $\mathcal{O}(1/\Lambda^2)$ Born contributions becoming negative at $p_T \sim 500$ GeV, indicating the failure of the EFT dimension-6 approximation for these parameters. A comparison of the blue and red lines on the RHS of Fig. 2 illustrates the huge numerical impact of including the full amplitude-squared, as compared to the $1/\Lambda^2$ truncation. Similarly, at $1/\Lambda^2$ the anomalous fermion coupling contribution is indistinguishable from the SM and their full effect occurs at the amplitude-squared level.

The LL contribution is shown on the LHS of Fig. 3 and at high p_T, we see the growth of the amplitude-squared in both the "3GB" and "Ferm" scenarios. The effects from anomalous gauge boson couplings and from anomalous fermion couplings are numerically very similar in the scenarios we have chosen here, and the effects cannot be separated by a measurement of W^+W^- production alone. As in the LT case, we see that truncating

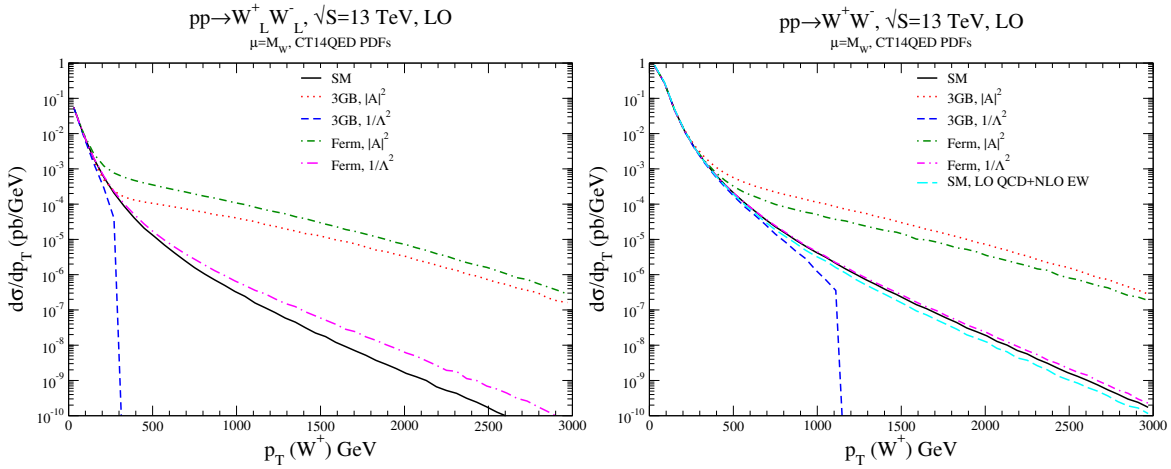

FIG. 3: Tree-level cross sections for $W_L^+W_L^-$ (LHS) and the sum of all polarizations (RHS) at the 13 TeV LHC in the SM and in the scenarios of Eq.(17). The curves labelled $|A|^2$ include the square of the dimension-6 amplitudes, while the curves labelled $1/\Lambda^2$ have the EFT result consistently truncated at $1/\Lambda^2$. The LL (LHS) and total (RHS) curves for the 3GB amplitude in the EFT should be truncated at $p_T \sim 350$ GeV, where the LL rate becomes negative and the EFT expansion fails. The SM curve on the RHS includes the complete set of electroweak corrections.

the 3GB rate at $\mathcal{O}(1/\Lambda^2)$ leads to negative cross sections at small p_T.

The unpolarized cross sections are shown on the RHS of Fig. 3. The green and red curves on the RHS of Fig. 3 demonstrate that the growth of the cross section at high p_T results from the square of the anomalous coupling contribution. This contribution is formally of dimension-8 and is potentially of the same size as the neglected dimension-8 contributions. The RHS of Fig. 3 also shows the effect of adding the complete electroweak corrections to the SM prediction [21]. Even at $p_T \sim 3$ TeV, these corrections are small and so are neglected in the rest of this work.

As the previous discussion indicates, for the parameter point "3GB" the EFT approximation begins to fail at a W^+ transverse momentum of a few 100 GeV. However, where the EFT fails strongly depends the values of the anomalous triple gauge boson couplings. We consider another scenario:

$$\text{3GB}' : \qquad \delta g_1^Z = 0.00452,\ \delta\kappa^Z = 0.0239,\ \lambda^Z = 0.0163,$$

where the anomalous fermionic couplings are set to zero. Figure 4 compares the "3GB"

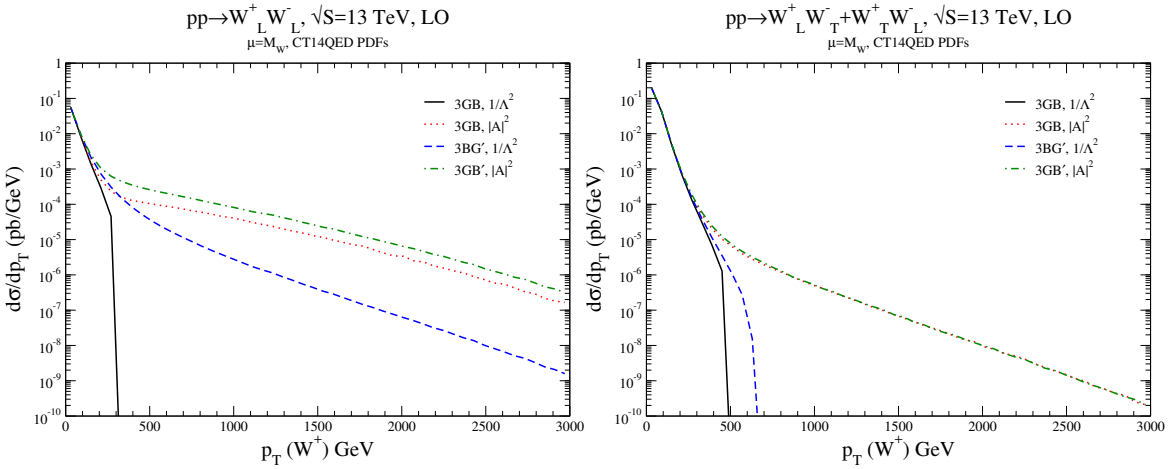

FIG. 4: Tree-level cross sections for $W_L^+W_L^-$ (LHS) and $W_T^+W_L^- + W_L^+W_T^-$ (RHS) at the 13 TeV LHC in the "3GB" and "3GB′" scenarios of Eqs.(17,21). The curves labelled $|A|^2$ include the square of the dimension-6 amplitudes, while the curves labelled $1/\Lambda^2$ have the EFT result consistently truncated at $1/\Lambda^2$. For the "3GB" amplitude, the LL (LHS) curves should be truncated at $p_T \sim 350$ GeV and the LT (RHS) at $p_T \sim 500$ GeV, where the respective rate becomes negative and the EFT expansion fails. For the "3GB′" amplitude, the LT(RHS) curves are negative and should be truncated at $p_T \sim 650$ GeV, while the LL (LHS) rates do not go negative.

and "3GB′" scenarios at leading order. The LL production rate (LHS) in the "3GB′" scenario does not go negative and the EFT approximation is valid. This is to be compared to the "3GB" scenario where the EFT approximation fails at $p_T \sim 350$ GeV. For the LT case, the "3GB′" rate becomes negative at $p_T \sim 650$ GeV. This extends the validity of the EFT by ~ 150 GeV above where the "3GB" scenario fails.

B. NLO QCD Effects

The lowest order results can potentially be significantly changed by the inclusion of higher order QCD and EW effects. The EFT contributions parametrized in the Lagrangians of Eqs. (2) and (3) do not affect the structure of the QCD corrections. We can therefore include the NLO QCD effects to $\mathcal{O}(\alpha_s)$ by calculating the virtual and real contributions using the SM Lagrangian supplemented by the anomalous coupling terms, using the same structure for the Catani-Seymour dipoles [39] to cancel the infrared divergences

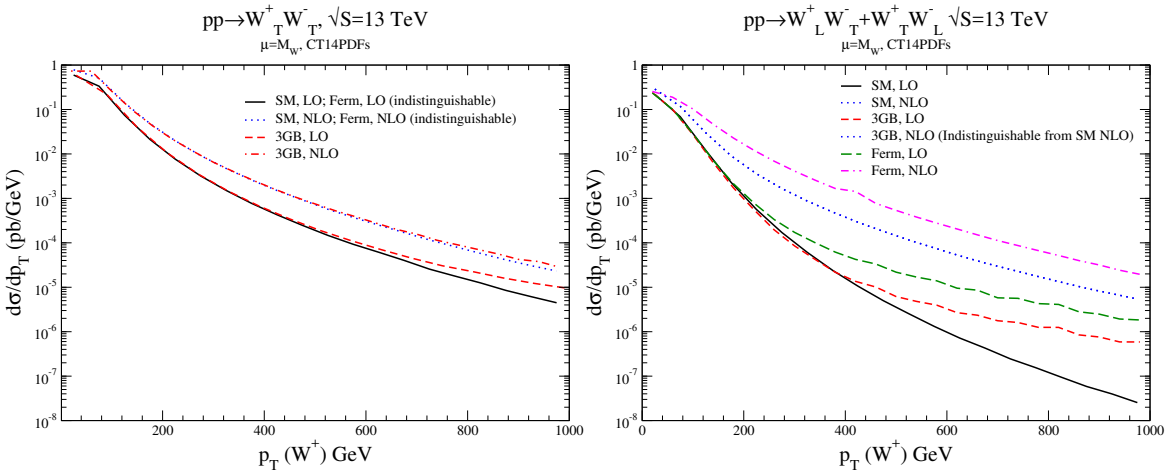

FIG. 5: Comparison of LO and NLO QCD results for the SM and the "3GB" and "Ferm" scenarios defined in Eqs. (17), (19), and (20) for $W_T^+W_T^-$ (LHS) and $W_L^\pm W_T^\mp$ (RHS) productions. This figure includes the complete amplitude-squared.

as in the SM calculation. Hence we use the same setup as in Ref. [21] in which the details for the SM calculation are given. The amplitudes for the NLO QCD EFT contributions have been calculated using `FeynArts-3.7` [40] and `FormCalc-7.5` [41], based on our Model File for `FeynArts` for the anomalous couplings developed with the help of `FeynRules` [42][5]. The one-loop integrals have been implemented with `LoopTools-2.12` [41, 43] and the Born and virtual pieces have been cross-checked against an independent analytical calculation. Since the SM NLO EW corrections are small (see RHS of Fig. 3), we do not anticipate that the $\mathcal{O}(\delta g_{\rm EFT}\alpha)$ corrections[6] will be significant enough to deserve further scrutiny.

The LO results presented in the previous section have emphasized that the consistent EFT expansion up to $\mathcal{O}(1/\Lambda^2)$ can give sizable deviations from the SM distributions, especially for the 3GB operators (see Fig. 3), and that the EFT expansion truncated at $\mathcal{O}(1/\Lambda^2)$ typically fails at moderate p_T. The large effects from anomalous couplings result from the terms which are quadratic in the squared-amplitudes. This observation is not significantly altered by the inclusion of the NLO QCD corrections.

Figs. 5 and 6 show the LO and NLO QCD corrected results for the TT, TL+LT, LL, and

[5] The open-access version of our code as well as the code giving the EW corrections in the SM and developed in Ref. [21] are included in https://quark.phy.bnl.gov/Digital_Data_Archive/dawson/ww_17.

[6] $\delta g_{\rm EFT}$ is here generically the deviation of any coupling from its SM value.

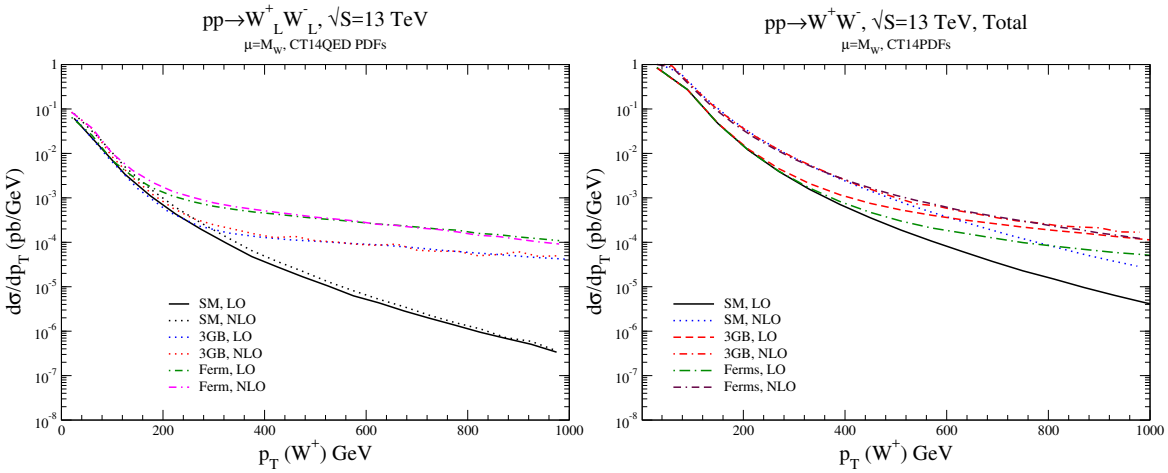

FIG. 6: Comparison of LO and NLO QCD results for the SM and the "3GB" and "Ferm" scenarios defined in Eqs. (17), (19), and (20) for $W_L^+W_L^-$ (LHS) and unpolarized W^+W^- (RHS) productions. This figure includes the complete amplitude-squared.

total W^+W^- p_T spectrums for the "3GB" and "Ferm" scenarios of the previous section compared with the SM, when the total amplitudes are squared and all terms included. The TT cross section has significant K factors for the 3GB anomalous couplings, the "Ferm" scenario, and the SM. At NLO the SM and "Ferm" scenarios are indistinguishable and most of the 3GB excess is erased (LHS of Fig. 5). The LT polarization (RHS of Fig. 5) displays a large K-factor in the SM, "3GB", and "Ferm" scenarios, larger than that for either the TT or LL polarizations. This behavior is due to the fact that the SM amplitude-squared is suppressed by $\frac{M_W^2}{s}$, enhancing naturally the K-factor. At NLO in the LT channel, the enhancement of the rate in the "Ferm" scenario over the SM at high p_T persists; however, the "3GB" spectrum is indistinguishable from the SM. Including the QCD corrections in the LT channel is clearly critical for obtaining accurate results. Interestingly, in the LL channel, the NLO QCD corrections in all scenarios are small and the excesses remain. Finally, we consider the total rate (RHS of Fig. 5). The SM NLO QCD corrections are dominated by the TT channel, as could be espected by the large Sudakov logarithms coming from a hard p_T jet radiating off a soft W boson; the quarks being massless, the longitudinal W bosons decouple at high energy. At NLO, the effects of the "Ferm" and "3GB" scenarios are largely similar, and the enhancement relative to the SM stays intact. The "Ferm" scenario and SM have significant K-factors, while the NLO

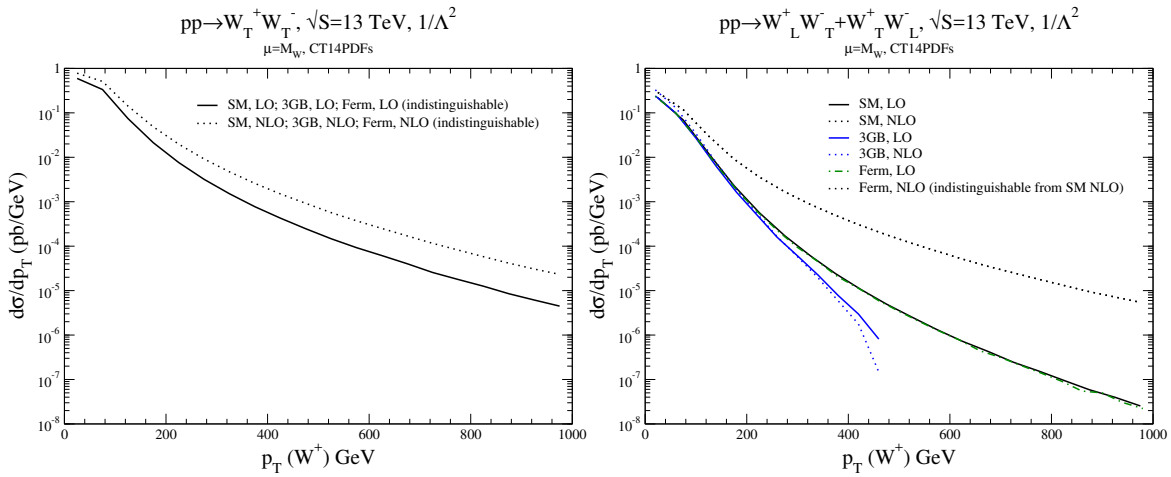

FIG. 7: Comparison of LO and NLO QCD results (LHS: TT polarization; RHS: LT+TL polarization) for the SM and the "3GB" and "Ferm" scenarios defined in Eqs.(17), (19), and (20), truncated at $\mathcal{O}(1/\Lambda^2)$. The 3GB LT curve is truncated at $p_T \sim 500$ GeV, since the LO cross section becomes negative at this point, signaling a breakdown in the EFT $\mathcal{O}(1/\Lambda^2)$ approximation.

corrections to 3GB are unimportant at high p_T. Since the LL configuration dominates the "3GB" scenario at high p_T, this conclusion was expected already from the analysis of the LL curves. It should be noted that the effects of the fermion anomalous couplings are largest in the LL polarization. Hence, sensitivity to these couplings would be greatly enhanced by performing an LL polarized analysis.

In Figs. 7 and 8, we show the comparison of the SM, "3GB" and "Ferm" scenarios at LO and NLO QCD, truncated at $\mathcal{O}(1/\Lambda^2)$. We have cut off the curves at the points where the LO rates go negative for each polarization in this approximation, since the EFT is no longer valid. It is immediately apparent that the effects of the anomalous couplings are small in the TT and LT polarizations in this EFT approximation and that the entire effect in Fig. 5 is from the contributions quadratic in the anomalous couplings. In the LL polarization (LHS of Fig. 8), we see that as before, the large enhancements seen earlier also arise from terms quadratic in the anomalous couplings, although the small LO effect of the anomalous fermion couplings at high p_T does remain at NLO. The RHS of Fig. 8 reflects the dominance of the TT polarization and illustrates the necessity of extracting polarized contributions. It also shows that the breakdown of the EFT $\mathcal{O}(1/\Lambda^2)$ expansion

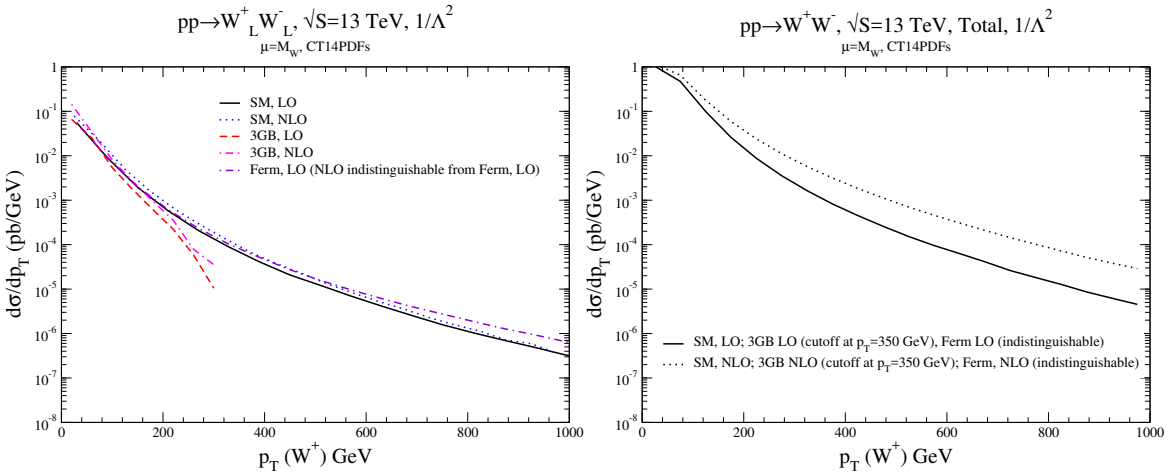

FIG. 8: Comparison of LO and NLO QCD results (LHS: LL polarization; RHS: unpolarized results) for the SM and the "3GB" and "Ferm" scenarios defined in Eqs.(17), (19), and (20), truncated at $\mathcal{O}(1/\Lambda^2)$. The 3GB curves are truncated at $p_T \sim 350$ GeV, since the LO LL cross section becomes negative at this point, signaling a breakdown in the EFT $\mathcal{O}(1/\Lambda^2)$ approximation.

happens much earlier than would be expected by the global fit analysis using σ^{cut} of Eq. (15).

IV. CONCLUSIONS

We have considered the effects of including both anomalous fermion and anomalous gauge boson interactions to the p_T spectrum of W^+W^- pair production. At LO QCD, the inclusion of even small anomalous fermion couplings can significantly affect the fits extracted by ATLAS and CMS. This observation has supported the need for global fits to the spectrum of EFT couplings. When the NLO QCD corrections are included, however, the sensitivity to anomalous fermion couplings in W^+W^- pair production diminishes; although, a polarized analysis in the longitudinal-longitudinal mode could enhance sensitivity to these couplings. The effect of the NLO QCD corrections is largest in the channel with one longitudinal and one transverse gauge boson, since the SM rate is suppressed by M_W^2/s in the high energy limit. The NLO EW corrections are small and do not affect the fits to the anomalous couplings. We have also re-iterated the well known observation that the sensitivity to anomalous couplings in W^+W^- pair production results almost entirely

from contributions quadratic in the dimension-6 EFT couplings. This is not altered by the inclusion of NLO QCD corrections.

The decays of the W bosons to fermion pairs are not included in our analysis. It should be noted that when the decays of the W bosons are considered, different W helicities can interfere. It was shown in Ref. [2] that the W helicities can be extracted in hadronic collisions by measuring the azimuthal angle between the plane of the W decay products and the plane of the incoming protons and virtual W's. This idea has been used recently to develop observables that are sensitive to the interference between the SM and BSM helicity amplitudes in WZ and $W\gamma$ production [44, 45]. This is the subject of on-going study for the W^+W^- case.

Acknowledgments

SD is supported by the United States Department of Energy under Grant Contract DE-SC0012704 and is grateful to the University of Tübingen, where this work was started. IML was supported in part by the University of Kansas General Research Fund allocation 2302091. J.B. is supported by the Kepler Center of the University of Tübingen and in part by the German Research Foundation (DFG) through the grant JA 1954/1 . Parts of this work were performed thanks to the support of the State of Baden-Württemberg through bwHPC and the DFG through the grant no. INST 39/963-1 FUGG. Digital data related to our results can be found at https://quark.phy.bnl.gov/Digital_Data_Archive/dawson/ww_17.

Appendix A: Helicity Amplitudes for $q\bar{q} \to W^+W^-$

From Ref. [3], for the process $\bar{q}_s q_{s'} \to W^+_\lambda W^-_{\lambda'}$, the leading order helicity amplitudes are,

$$\mathcal{A}_{ss'\lambda\lambda'} \;=\; \sqrt{2}\widetilde{\mathcal{A}}_{ss'\lambda\lambda'}\widetilde{d}_{ss'\lambda\lambda'}(-1)^{\Delta\lambda}, \tag{A1}$$

where $\Delta s = (s - s')/2$, $\Delta\lambda = (\lambda - \lambda')$, $J = \max(|\Delta s|, |\Delta\lambda|)$. We can further decompose the amplitudes, separating out the information from the quark couplings,

$$\begin{aligned}
\widetilde{\mathcal{A}}_{-+\lambda\lambda'} &= g_Z^2 c_W^2 \left(g_R^{Zq} + \delta g_R^{Zq}\right) \beta_W \frac{s}{s - M_Z^2} A^Z_{\lambda\lambda'} + e^2 Q_q \beta_W A^\gamma_{\lambda\lambda'} \\
&= e^2 Q_q \beta_W \left(A^\gamma_{\lambda\lambda'} - \frac{s}{s - M_Z^2} A^Z_{\lambda\lambda'}\right) + g^2 \delta g_R^{Zq} \beta_W \frac{s}{s - M_Z^2} A^Z_{\lambda\lambda'} \qquad \text{(A2)} \\
\widetilde{\mathcal{A}}_{+-\lambda\lambda'} &= g_Z^2 c_W^2 \left(g_L^{Zq} + \delta g_L^{Zq}\right) \beta_W \frac{s}{s - M_Z^2} A^Z_{\lambda\lambda'} + e^2 Q_q \beta_W A^\gamma_{\lambda\lambda'} + 2\, T_3^q \frac{g^2}{\beta_W} \left(1 + \delta g_L^W\right)^2 A^W_{\lambda\lambda'},
\end{aligned}$$

with $\beta_W = \sqrt{1 - 4M_W^2/s}$.

The A^Z, A^γ and A^W coefficients are ($V = \gamma, Z$ and $\delta g_1^\gamma = 0$):

$$\begin{aligned}
A^V_{00} &= \frac{s}{2M_W^2} + 1 + \left(\delta g_1^V + \delta\kappa^V \frac{s}{2M_W^2}\right), \\
A^W_{00} &= -\frac{s}{4M_W^2} + \frac{4M_W^2}{s} \frac{1}{1 + \beta_W^2 - 4\, T_3^q\, \beta_W \cos\theta}, \\
A^V_{+0} &= A^V_{0+} = A^V_{-0} = A^V_{0-} = \frac{\sqrt{s}}{M_W} \left(1 + \frac{1}{2}\left(\delta g_1^V + \delta\kappa^V + \lambda^V\right)\right), \\
A^W_{+0} &= A^W_{0-} = \frac{\sqrt{s}}{M_W} \left(\frac{2M_W^2}{s} \frac{1}{1 + \beta_W^2 - 4\, T_3^q\, \beta_W \cos\theta} (1 - 2\, T_3^q\, \beta_W) - \frac{1}{2}\right), \\
A^W_{0+} &= A^W_{-0} = \frac{\sqrt{s}}{M_W} \left(\frac{2M_W^2}{s} \frac{1}{1 + \beta_W^2 - 4\, T_3^q\, \beta_W \cos\theta} (1 + 2\, T_3^q\, \beta_W) - \frac{1}{2}\right), \\
A^V_{--} &= A^V_{++} = 1 + \delta g_1^V + \frac{s}{2M_W^2} \lambda^V, \\
A^W_{--} &= A^W_{++} = -\frac{1}{2} + \frac{2M_W^2}{s} \frac{1}{1 + \beta_W^2 - 4\, T_3^q\, \beta_W \cos\theta}, \\
A^V_{+-} &= A^V_{-+} = 0, \\
A^W_{+-} &= A^W_{-+} = 2\sqrt{2}\, T_3^q\, \beta_W \frac{1}{1 + \beta_W^2 - 4\, T_3^q\, \beta_W \cos\theta}. \qquad \text{(A3)}
\end{aligned}$$

The necessary Wigner-D functions are,

$$\begin{aligned}
\widetilde{d}_{-1,+1,0,0} &= \widetilde{d}_{-1,+1,-1,-1} = \widetilde{d}_{-1,+1,+1,+1} = -\widetilde{d}_{+1,-1,0,0} = -\widetilde{d}_{+1,-1,-1,-1} = -\widetilde{d}_{+1,-1,+1,+1} = \frac{1}{\sqrt{2}} \sin\theta, \\
\widetilde{d}_{-1,+1,0,+1} &= \widetilde{d}_{-1,+1,-1,0} = \widetilde{d}_{+1,-1,0,-1} = \widetilde{d}_{+1,-1,+1,0} = -\frac{1}{2}\left(1 + \cos\theta\right), \\
\widetilde{d}_{-1,+1,+1,0} &= \widetilde{d}_{-1,+1,0,-1} = \widetilde{d}_{+1,-1,-1,0} = \widetilde{d}_{+1,-1,0,+1} = -\frac{1}{2}\left(1 - \cos\theta\right), \\
\widetilde{d}_{+1,-1,+1,-1} &= -\widetilde{d}_{-1,+1,-1,+1} = \frac{1}{2}\left(1 + \cos\theta\right)\sin\theta, \\
\widetilde{d}_{-1,+1,+1,-1} &= -\widetilde{d}_{+1,-1,-1,+1} = \frac{1}{2}\left(1 - \cos\theta\right)\sin\theta. \qquad \text{(A4)}
\end{aligned}$$

[1] K. J. F. Gaemers and G. J. Gounaris, "Polarization Amplitudes for $e^+e^- \to W^+W^-$ and $e^+e^- \to ZZ$," *Z. Phys.* **C1** (1979) 259.

[2] M. J. Duncan, G. L. Kane, and W. W. Repko, "WW Physics at Future Colliders," *Nucl. Phys.* **B272** (1986) 517–559.

[3] K. Hagiwara, R. D. Peccei, D. Zeppenfeld, and K. Hikasa, "Probing the Weak Boson Sector in $e^+e^- \to W^+W^-$," *Nucl. Phys.* **B282** (1987) 253–307.

[4] **DELPHI, OPAL, LEP Electroweak, ALEPH, L3** Collaboration, S. Schael *et al.*, "Electroweak Measurements in Electron-Positron Collisions at W-Boson-Pair Energies at LEP," *Phys. Rept.* **532** (2013) 119–244, arXiv:1302.3415 [hep-ex].

[5] A. Falkowski and F. Riva, "Model-independent precision constraints on dimension-6 operators," *JHEP* **02** (2015) 039, arXiv:1411.0669 [hep-ph].

[6] A. Butter, O. J. P. Eboli, J. Gonzalez-Fraile, M. C. Gonzalez-Garcia, T. Plehn, and M. Rauch, "The Gauge-Higgs Legacy of the LHC Run I," *JHEP* **07** (2016) 152, arXiv:1604.03105 [hep-ph].

[7] L. Berthier, M. Bjorn, and M. Trott, "Incorporating doubly resonant $W^\pm$ data in a global fit of SMEFT parameters to lift flat directions," *JHEP* **09** (2016) 157, arXiv:1606.06693 [hep-ph].

[8] J. de Blas, M. Ciuchini, E. Franco, S. Mishima, M. Pierini, L. Reina, and L. Silvestrini, "Electroweak precision observables and Higgs-boson signal strengths in the Standard Model and beyond: present and future," *JHEP* **12** (2016) 135, arXiv:1608.01509 [hep-ph].

[9] Z. Zhang, "Time to Go Beyond Triple-Gauge-Boson-Coupling Interpretation of W Pair Production," *Phys. Rev. Lett.* **118** no. 1, (2017) 011803, arXiv:1610.01618 [hep-ph].

[10] **CMS** Collaboration, V. Khachatryan *et al.*, "Measurement of the $\mathrm{W^+W^-}$ cross section in pp collisions at $\sqrt{s} = 8$ TeV and limits on anomalous gauge couplings," *Eur. Phys. J.* **C76** no. 7, (2016) 401, arXiv:1507.03268 [hep-ex].

[11] **ATLAS** Collaboration, G. Aad *et al.*, "Measurement of total and differential W^+W^- production cross sections in proton-proton collisions at $\sqrt{s} = 8$ TeV with the ATLAS detector and limits on anomalous triple-gauge-boson couplings," *JHEP* **09** (2016) 029,

arXiv:1603.01702 [hep-ex].

[12] W. Buchmuller and D. Wyler, "Effective Lagrangian Analysis of New Interactions and Flavor Conservation," *Nucl. Phys.* **B268** (1986) 621–653.

[13] B. Grzadkowski, M. Iskrzynski, M. Misiak, and J. Rosiek, "Dimension-Six Terms in the Standard Model Lagrangian," *JHEP* **10** (2010) 085, arXiv:1008.4884 [hep-ph].

[14] A. Azatov, R. Contino, C. S. Machado, and F. Riva, "Helicity selection rules and noninterference for BSM amplitudes," *Phys. Rev.* **D95** no. 6, (2017) 065014, arXiv:1607.05236 [hep-ph].

[15] A. Falkowski, M. Gonzalez-Alonso, A. Greljo, D. Marzocca, and M. Son, "Anomalous Triple Gauge Couplings in the Effective Field Theory Approach at the LHC," *JHEP* **02** (2017) 115, arXiv:1609.06312 [hep-ph].

[16] T. Gehrmann, M. Grazzini, S. Kallweit, P. Maierhofer, A. von Manteuffel, S. Pozzorini, D. Rathlev, and L. Tancredi, "W^+W^- Production at Hadron Colliders in Next to Next to Leading Order QCD," *Phys. Rev. Lett.* **113** no. 21, (2014) 212001, arXiv:1408.5243 [hep-ph].

[17] M. Grazzini, S. Kallweit, S. Pozzorini, D. Rathlev, and M. Wiesemann, "W^+W^- production at the LHC: fiducial cross sections and distributions in NNLO QCD," *JHEP* **08** (2016) 140, arXiv:1605.02716 [hep-ph].

[18] S. Dawson, P. Jaiswal, Y. Li, H. Ramani, and M. Zeng, "Resummation of jet veto logarithms at $\mathrm{N^3LL}_a$ + NNLO for W^+W^- production at the LHC," *Phys. Rev.* **D94** no. 11, (2016) 114014, arXiv:1606.01034 [hep-ph].

[19] K. Hamilton, T. Melia, P. F. Monni, E. Re, and G. Zanderighi, "Merging WW and WW+jet with MINLO," *JHEP* **09** (2016) 057, arXiv:1606.07062 [hep-ph].

[20] A. Bierweiler, T. Kasprzik, and J. H. Kuhn, "Vector-boson pair production at the LHC to $\mathcal{O}(\alpha^3)$ accuracy," *JHEP* **12** (2013) 071, arXiv:1305.5402 [hep-ph].

[21] J. Baglio, L. D. Ninh, and M. M. Weber, "Massive gauge boson pair production at the LHC: a next-to-leading order story," *Phys. Rev.* **D88** (2013) 113005, arXiv:1307.4331 [hep-ph]. [Erratum: Phys. Rev.D94,no.9,099902(2016)].

[22] B. Biedermann, M. Billoni, A. Denner, S. Dittmaier, L. Hofer, B. Jaeger, and L. Salfelder, "Next-to-leading-order electroweak corrections to $pp \to W^+W^- \to 4$ leptons at the LHC," *JHEP* **06** (2016) 065, arXiv:1605.03419 [hep-ph].

[23] B. Biedermann, A. Denner, S. Dittmaier, L. Hofer, and B. Jaeger, "Next-to-leading order electroweak corrections to $pp \to \mu^+\mu^- e^+ e^- + X$ at the LHC Collider," *PoS* **RADCOR2015** (2016) 020.

[24] B. Biedermann, A. Denner, S. Dittmaier, L. Hofer, and B. Jaeger, "Next-to-leading-order electroweak corrections to the production of four charged leptons at the LHC," *JHEP* **01** (2017) 033, arXiv:1611.05338 [hep-ph].

[25] S. Kallweit, J. M. Lindert, S. Pozzorini, and M. Schonherr, "NLO QCD+EW predictions for $2\ell 2\nu$ diboson signatures at the LHC," arXiv:1705.00598 [hep-ph].

[26] L. J. Dixon, Z. Kunszt, and A. Signer, "Vector boson pair production in hadronic collisions at order α_s : Lepton correlations and anomalous couplings," *Phys. Rev.* **D60** (1999) 114037, arXiv:hep-ph/9907305 [hep-ph].

[27] A. Falkowski, "Effective field theory approach to LHC Higgs data," *Pramana* **87** no. 3, (2016) 39, arXiv:1505.00046 [hep-ph].

[28] I. Brivio and M. Trott, "Scheming in the SMEFT... and a reparameterization invariance!," arXiv:1701.06424 [hep-ph].

[29] L. Berthier and M. Trott, "Towards consistent Electroweak Precision Data constraints in the SMEFT," *JHEP* **05** (2015) 024, arXiv:1502.02570 [hep-ph].

[30] R. S. Chivukula and H. Georgi, "Composite Technicolor Standard Model," *Phys. Lett.* **B188** (1987) 99–104.

[31] G. D'Ambrosio, G. F. Giudice, G. Isidori, and A. Strumia, "Minimal flavor violation: An Effective field theory approach," *Nucl. Phys.* **B645** (2002) 155–187, arXiv:hep-ph/0207036 [hep-ph].

[32] R. Alonso, E. E. Jenkins, A. V. Manohar, and M. Trott, "Renormalization Group Evolution of the Standard Model Dimension Six Operators III: Gauge Coupling Dependence and Phenomenology," *JHEP* **04** (2014) 159, arXiv:1312.2014 [hep-ph].

[33] A. Biekotter, J. Brehmer, and T. Plehn, "Extending the limits of Higgs effective theory," *Phys. Rev.* **D94** no. 5, (2016) 055032, arXiv:1602.05202 [hep-ph].

[34] **CMS** Collaboration, A. M. Sirunyan *et al.*, "Search for anomalous couplings in boosted WW/WZ $\to \ell\nu\mathrm{q}\bar{\mathrm{q}}$ production in proton-proton collisions at $\sqrt{s} = 8$ TeV," *Phys. Lett.* **B772** (2017) 21–42, arXiv:1703.06095 [hep-ex].

[35] N. Moshtagh, "Minimum volume enclosing ellipsoids," tech. rep., University of

Pennsylvania, 2009.

[36] L. Berthier and M. Trott, "Consistent constraints on the Standard Model Effective Field Theory," *JHEP* **02** (2016) 069, arXiv:1508.05060 [hep-ph].

[37] C. Schmidt, J. Pumplin, D. Stump, and C. P. Yuan, "CT14QED parton distribution functions from isolated photon production in deep inelastic scattering," *Phys. Rev.* **D93** no. 11, (2016) 114015, arXiv:1509.02905 [hep-ph].

[38] A. Buckley, J. Ferrando, S. Lloyd, K. Nordström, B. Page, M. Rüfenacht, M. Schönherr, and G. Watt, "LHAPDF6: parton density access in the LHC precision era," *Eur. Phys. J.* **C75** (2015) 132, arXiv:1412.7420 [hep-ph].

[39] S. Catani and M. H. Seymour, "A General algorithm for calculating jet cross-sections in NLO QCD," *Nucl. Phys.* **B485** (1997) 291–419, arXiv:hep-ph/9605323 [hep-ph]. [Erratum: Nucl. Phys.B510,503(1998)].

[40] T. Hahn, "Generating Feynman diagrams and amplitudes with FeynArts 3," *Comput. Phys. Commun.* **140** (2001) 418–431, arXiv:hep-ph/0012260 [hep-ph].

[41] T. Hahn and M. Perez-Victoria, "Automatized one loop calculations in four-dimensions and D-dimensions," *Comput. Phys. Commun.* **118** (1999) 153–165, arXiv:hep-ph/9807565 [hep-ph].

[42] A. Alloul, N. D. Christensen, C. Degrande, C. Duhr, and B. Fuks, "FeynRules 2.0 - A complete toolbox for tree-level phenomenology," *Comput. Phys. Commun.* **185** (2014) 2250–2300, arXiv:1310.1921 [hep-ph].

[43] G. J. van Oldenborgh, "FF: A Package to evaluate one loop Feynman diagrams," *Comput. Phys. Commun.* **66** (1991) 1–15.

[44] A. Azatov, J. Elias-Miro, Y. Reyimuaji, and E. Venturini, "Novel measurements of anomalous triple gauge couplings for the LHC," arXiv:1707.08060 [hep-ph].

[45] G. Panico, F. Riva, and A. Wulzer, "Diboson Interference Resurrection," arXiv:1708.07823 [hep-ph].